Geomechanics and Geoengineering: An International Journal
Vol. 1, No. 1, March 2006, 3–11

Estimation of maximum mud pressure in purely cohesive material during directional drilling

H. W. XIA and I. D. MOORE*

GeoEngineering Centre at Queen's-RMC, Queen's University, Kingston, ON K7L 3N6, Canada

(Received 31 October 2005; in final form 26 January 2006)

Directional drilling requires the use of drilling mud to stabilize the borehole and return cuttings to the ground surface. High mud pressure can result in mud loss, ground heave, damage to buried infrastructure, and other serious problems as a result of either hydrofracture or blowout of the soil surrounding the borehole. First, past research on two ground failure mechanisms is reviewed. A new approach is introduced to estimate maximum mud pressure using a cavity expansion solution, where the non-unit lateral earth pressure coefficient at rest (K_0) is explicitly considered. Finite-element analyses demonstrate that the new approach provides effective estimates of the extent of the plastic zone around the borehole under different geostatic stress conditions. Control of mud pressures to prevent the zone of shear failure extending more than halfway to the ground surface produces a reserve capacity of 20–30% against blowout. An examination of hydrofracture versus blowout indicates that blowout is the most likely mode of mud loss in normally and lightly overconsolidated clays. Hydrofracture is the expected cause of mud loss in heavily overconsolidated clays when the coefficient of lateral earth pressure exceeds 1.8.

Keywords: Horizontal directional drilling; Hydraulic fracturing; Blowout; Maximum allowable mud pressure

1. Introduction

Over the past two decades, directional drilling has been developed as an alternative to traditional cut-and-cover methods for installation or replacement of buried pipes. Motivating factors for the use of directional drilling include the potential of cost savings, greater flexibility of operations, and greatly reduced impact on the adjacent environment, especially when crossing crowded urban areas, rivers, and sensitive or protected environments.

The directional drilling process includes main three stages: pilot hole boring, pilot hole reaming, and pull-back (Allouche *et al.* 1998). Drilling mud is introduced at the drill head from the beginning of the pilot boring process and is present in all stages of drilling. The main purposes for the drilling mud are to transport excavated drill cuttings back to the ground surface, to clean and cool the drill bit, to reduce sidewall resistance when the pipe is dragged through the borehole, and to prevent the borehole from collapsing (Ariaratnam and Allouche 2000). Low mud pressure may cause borehole contraction or borehole collapse, and these can increase the friction force or block the borehole and make the pilot hole reaming and pull-back operations more difficult. High mud pressures may result in mud flow from the borehole following tensile failure (hydraulic fracturing or 'hydrofracture') or shear failure (blowout) of the soil in the vicinity of the borehole. Engineers and contractors responsible for directional drilling projects need guidelines for limiting mud pressures to prevent these difficulties.

Past investigations of two different mud loss mechanisms and maximum allowable mud pressure are reviewed. A new approach is then developed to estimate the development of shear failure around the borehole and the maximum allowable mud pressures. The new approach is compared with the blowout equation introduced by Arends (2003) as well as with finite-element analyses. The study concludes with a review of limiting mud pressures and the mechanisms controlling mud loss for both normally consolidated and overconsolidated clays.

2. Literature review

This review examines different approaches proposed in the literature to calculate the allowable mud pressure during directional drilling. Two mechanisms have been identified as having the potential to cause ground failure and mud loss. The first is associated with generalized shear failure in the soil and loss of confinement around the borehole, the so called 'blowout' mechanism (figure 1(a)). Arends (2003) suggested that the maximum safe mud pressure to prevent blowout is the pressure that brings the zone of shear failure in the soil (the plastic zone) halfway to the ground surface. Alternatively, 'hydraulic fracturing' (figure 1(b)) or tensile failure of the soil can occur when the minor principal stress mobilizes the full tensile strength of the soil, which is conservatively assumed to be zero, followed

*Corresponding author. Email: moore@civil.queensu.ca

Geomechanics and Geoengineering: An International Journal
ISSN 1748-6025 print/ISSN 1748-6033 online © 2006 Taylor & Francis
http://www.tandf.co.uk/journals
DOI: 10.1080/17486020600604024

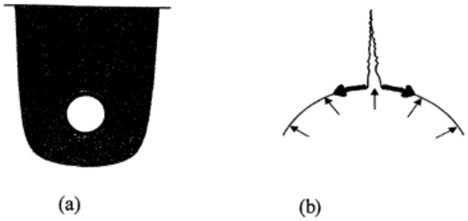

Figure 1. Two mechanisms of soil failure leading to mud loss: (a) shear failure (blowout); (b) tensile failure (hydraulic fracturing).

by propagation to the ground surface (Kennedy *et al.* 2004a). Moore (2005) suggested that the maximum allowable mud pressure to prevent mud loss by hydrofracture is the pressure that initiates tensile stresses in the soil.

2.1 *Shear failure mechanism*

Carter *et al.* (1986) derived closed-form solutions for the expansion of cylindrical cavities in an ideal cohesive–frictional material. The material is assumed to be isotropic, but could be elastic and plastic. It obeys Hooke's law until onset of yield, which is determined by the Mohr–Coulomb criterion. The maximum pressure is taken as the pressure when large radial displacement or plastic expansion occurs. Some researchers (Mori and Tamura 1987, Panah and Yanagisawa 1989) have studied the shear failure mechanism in soils using laboratory experiments. They concluded that shear failure of the soil is the cause of mud loss, and that fracturing initiates when the stresses of a soil element around the borehole reach the Mohr–Coulomb strength envelope. They also concluded that the maximum borehole pressure should be set as the pressure which causes the initiation of shear failure in the soil. These procedures lead to very safe solutions since they do not make use of the strength of the remaining soil surrounding the borehole; significant increases in the mud pressure are required to expand the radius of the plastic zone up to the ground surface.

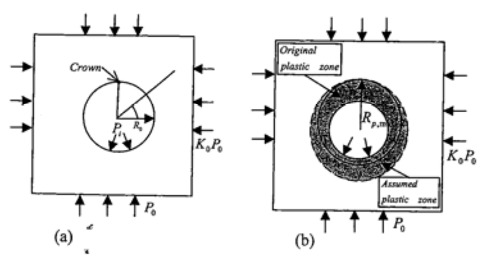

Figure 2. Definition of the problem and geometry of the plastic zone: (a) borehole in a solid under orthotropic stress; (b) geometrical conditions for the new approach.

Arends (2003) reported on the closed-form solution used by Keulen (2001) at Delft University to estimate the maximum allowable mud pressure during directional drilling. This closed-form solution was originally developed by Vesic *et al.* (1972) based on cavity expansion theory, and is generally called the 'Delft equation' by the trenchless technology community (this name will also be used subsequently in this paper). The assumptions of this theoretical solution can be summarized as follows: the borehole is axially symmetric, and the soil medium is homogeneous, isotropic, and of infinite size. The medium was assumed to be in an isotropic initial stress condition (i.e. $K_0 = 1$) and its response was modelled as elastic until the onset of shear failure, which was defined using the Mohr–Coulomb failure criterion (based on cohesion and frictional angle). Increments of elastic deformation were calculated using Hooke's law, elastic deformations in the plastic zone were neglected, and it was assumed that the volume change in the plastic zone was zero.

The maximum allowable mud pressure is expressed as follows:

$$P_{\max} = P'_{\max} + u \tag{1}$$

$$P'_{\max} = \left(\sigma'_0(1+\sin\phi) + c\cos\phi + c\cot\phi\right)\left\{\left(\frac{R_0}{R_{p,\max}}\right)^2 + \frac{(\sigma'_0\sin\phi + c\cos\phi)}{G}\right\}^{\frac{-\sin\phi}{1+\sin\phi}} - c\cot\phi \tag{2}$$

where $P_{\max}$ is the maximum allowable mud pressure, u is the initial *in situ* pore pressure, $P'_{\max}$ is the maximum allowable effective mud pressure, σ'_0 is the initial effective stress, ϕ is the internal friction angle, c is the cohesion, R_0 is the initial radius of the borehole, $R_{p,\max}$ is the maximum allowable radius of the plastic zone, and G is the shear modulus.

For practical applications, Arends (2003) suggested that the maximum allowable radius of the plastic zone should be selected as half the cover depth for cohesive material. The Delft equation applies to frictional–cohesive soil and is expressed in terms of effective stresses. The focus of attention in the current paper is purely cohesive soils, and total stresses are employed.

2.2 *Hydraulic fracturing mechanism*

Bjerrum *et al.* (1972) introduced the concept of hydraulic fracturing, which can occur during *in situ* field permeability tests, to explain how those field tests overestimate the permeability of clayey soil. They concluded that the fracture initiates when the tensile effective circumferential stress exceeds the tensile strength of the material. Andersen *et al.* (1994) proposed an approach which was based on the general principle that fracture occurs when the minor principle effective stress become negative (i.e. tensile) with magnitude equal to or greater than the tensile strength of soil. In this approach, they emphasized the non-linearity of the stress–strain properties of soil, and the pore pressure changes in the soil induced by changes in total mean normal stress and shear stress. This approach indicated that failure pressure was controlled by the overconsolidated ratio (OCR). When the OCR was less than 4.0, a tensile failure mechanism was inferred.

Kennedy *et al.* (2004a,b) used finite-element analysis to examine the response of an elastic–plastic soil during boring under a range of different drilling mud pressures. They concluded that the initiation of a tensile fracture occurs at the crown of the borehole, where $K_0 < 1$, and at the spring-line, where $K_0 > 1$. The limiting mud pressure causing fracture initiation is estimated by considering how the tangential stress in the soil at the crown or spring-line of the borehole reduces to zero from the initial compressive stress of P_0 (making the conservative assumption that the tensile strength of the soil is zero). Elastic continuum theory was used to determine that fracture initiates when mud pressures reach P_{frac}, which is given by

$$P_{frac}/P_0 = (3K_0 - 1) \quad \text{for } K_0 < 1 \tag{3a}$$

and

$$P_{frac}/P_0 = (3 - K_0) \quad \text{for } K_0 > 1 \tag{3b}$$

provided that

$$P_{frac} < 2C_u. \tag{4}$$

Murdoch (1993a,b,c) used laboratory tests to study the character of the fracture face and fracture propagation from a vertical borehole. Criteria were established based on conventional linear fracture mechanics and fracture toughness was introduced as a factor to estimate the fracture pressure. However, fracture toughness is very difficult to measure in practice. Murdoch (1993a, 2002) demonstrated that the fracture pressure was dependent on the width of the slot and the water content of the soil, and that the fluid pressures needed to propagate the fracture reduce significantly after fracture initiation. During directional drilling, the mud pressures are generally sustained by the column of mud going back to the ground surface, and so fracture propagation is probably rapid once it commences. Therefore prevention of fracture initiation is the best approach to controlling hydrofracture and mud loss.

3. A new approach to estimating maximum mud pressure

Each of the two ground failure mechanisms controls the maximum allowable mud pressure for a specific range of circumstances. Moore (2005) used finite-element analysis to investigate the performance of the Delft equation, and found that it provides good estimates of the radius of the plastic zone if the coefficient of lateral earth pressure at rest (K_0) is equal to or close to unity (i.e. $K_0 > 0.85$) but that it overestimates the critical mud pressure for lower values of K_0. On the other hand, the solution obtained by Kennedy *et al.* (2004a,b) does not provide estimates of fracture pressures for all values of K_0 (they showed that tensile fracture does not occur once shear failure is iniatiated). Therefore a new approach for estimating maximum mud pressure due to shear failure in purely cohesive material has been developed and is reported here. This can be used to estimate the maximum mud pressure in those regions where the lateral earth pressure coefficient K_0 is not covered by the solutions reported by Kennedy *et al.* (2004a,b) or by axisymmetric cavity expansion, i.e. the Delft equation (Arends 2003).

The initial radius of the borehole is R_0 and the initial stresses around the borehole obey the Kirsch solution for stresses around a circular hole in an elastic plate. The pressure inside the borehole is then increased to a value P_i and the borehole radius is increased to R_i. In the initial part of loading it is assumed that soil exhibits a linear elastic response up to a certain pressure limit, defined using the Mohr–Coulomb failure criterion. After initial yielding, the soil is assumed to exhibit perfectly plastic behaviour, and a plastic zone develops around the borehole with a plastic radius R_e that travels outwards as the mud pressure applied within the borehole increases. Plane strain conditions in the axial direction are assumed. In this analysis, the convention is adopted that compressive stresses and strains are positive, as is usual in soil mechanics.

Before the commencement of shear failure (initial yield), the stress distribution in the elastic region is expressed as (Yu 2000)

$$\sigma_R = \frac{1}{2} \cdot P_0 \cdot \left\{ (1 + K_0) \cdot \left(1 - \frac{R_0^2}{R^2}\right) + (1 - K_0) \cdot \left(1 - \frac{4R_0^2}{R^2} + 3\frac{R_0^4}{R^4}\right) \right\} + P_i \cdot \frac{R_0^2}{R^2} \tag{5a}$$

$$\sigma_\theta = \frac{1}{2} \cdot P_0 \cdot \left\{ (1 + K_0) \cdot \left(1 + \frac{R_0^2}{R^2}\right) - (1 - K_0) \cdot \left(1 + 3\frac{R_0^4}{R^4}\right) \right\} - P_i \cdot \frac{R_0^2}{R^2} \tag{5b}$$

$$\tau_{R\theta} = \frac{1}{2} \cdot P_0 \cdot \left\{ (1 - K_0) \cdot \left(1 + 2\frac{R_0^2}{R^2} - 3\frac{R_0^4}{R^4}\right) \sin 2\theta \right\}. \tag{5c}$$

The boundary conditions are

$$\sigma_{RR}^{R=\infty} = \frac{1}{2}(P_0 + K_0 P_O) + \frac{1}{2}(K_0 P_0 - P_0)\cos 2\theta \tag{6a}$$

$$\sigma_{R\theta}^{R=\infty} = -\frac{1}{2}(P_0 + K_0 P_O)\sin 2\theta. \tag{6b}$$

Moore (2005) used finite-element analysis to study the development of the plastic zone for soils of various strengths and geometries. That study indicates that shear failure initiates at the crown of the borehole once internal mud pressure fully mobilizes the shear strength of the soil. The plastic zone grows as the mud pressure increases, and the furthest shear point in the plastic zone appears over the crown when $K_0 < 1$. Simplified geometry is used in the new procedure. The focus of attention is the point experiencing shear failure that is furthest from the borehole axis. Stresses at this point, which lies above the crown of the borehole ($R = R_i$, $\theta = 90°$), become

$$\sigma_R = P_i \tag{7a}$$

$$\sigma_\theta = (3K_0 - 1)P_0 - P_i. \tag{7b}$$

If hydraulic fracturing does not occur before the initiation of shear failure, an annular plastic zone is assumed to develop around the borehole, where

$$\sigma_R - \sigma_\theta = 2C_u. \tag{8}$$

Based on this failure criterion, the critical mud pressure P_i for initial yield at the crown of the borehole is

$$P_i = C_u + \frac{1}{2}(3K_0 - 1)P_0. \tag{9}$$

At the point ($R = R_e$, $\theta = 90°$), i.e. above the crown at the interface between the plastic zone and the elastic region, the stress distributions are given by

$$\sigma_R = P_e = C_u + \frac{1}{2}(3K_0 - 1)P_0 \tag{10}$$

where P_e is the radial stress across the interface. At the point ($R = R_e$, $\theta = 90°$), the stresses also satisfy the equilibrium equation

$$\frac{\partial \sigma_R}{\partial R} + \frac{\sigma_R - \sigma_\theta}{R} = 0. \tag{11}$$

Substituting equation (8) into equation (11) and integrating gives

$$\sigma_R = -2C_u \ln R + C. \tag{12}$$

where the constant C is determined by the internal wall boundary condition. The radial stress above the crown in the plastic zone can then be expressed as

$$\sigma_R = P_i + 2C_u \ln\left(\frac{R_i}{R}\right). \tag{13}$$

The point ($R = R_e$, $\theta = 90°$) at the interface between the plastic and elastic zones above the crown of the borehole is in an equilibrium state, and so the following condition is satisfied:

$$\sigma_R^{e} = \sigma_R^{p} \qquad \text{at} \qquad R = R_e, \theta = 90°$$

where the superscripts e and p denote the elastic and plastic regions, respectively. The radial pressure P_i at the internal wall can then be determined considering the above condition:

$$P_i = C_u + \frac{1}{2}(3K_0 - 1)P_0 - 2C_u \ln\left(\frac{R_i}{R_e}\right). \tag{14}$$

An axisymmetric cavity expansion model is used here to represent stresses at point ($R = R_e$, $\theta = 90°$) for the asymmetric problem (where $K_0 \neq 1$). This approach involves the following assumptions.

- The plastic zone is assumed to be axisymmetric (shaped like a doughnut); its outer radius is interpreted as the distance between the centre of the borehole and the furthest point in the soil experiencing shear failure ($R_e = R_{p,max}$).
- At each point on the interface between the plastic and elastic zones, the displacement has the same value as the furthest plastic point ($R = R_e$, $\theta = 90°$) above the crown of the borehole.
- Displacement is modelled as independent of the position angle θ, but dependent on the maximum plastic radius $R_{p,max}$.

Based on the above assumptions, the displacement at the interface between the assumed plastic and elastic zones is given by the elasticity solution:

$$u_{(Re)} = \frac{(P_e - P_0) \cdot R_{p,\max}^2}{2GR_{p,\max}} = \frac{(C_u + \frac{3}{2}(K_0 - 1)P_0)R_{p,\max}}{2G} \tag{15}$$

No volume change ($\Delta V = 0$) is expected in the plastic zone during deformations experienced by this purely cohesive material (which should respond in an undrained condition); hence

$$\pi\left(R_{p,\max}^2 - R_i^2\right) = \pi\left((R_{p,\max} - u_{Re})^2 - R_0^2\right) \tag{16}$$

where $R_{p,max}$ is the distance from the centre of the borehole to the furthest shear failure point, R_i is the current borehole radius, U_{Re} is the displacement at the interface of the plastic and elastic zones, and R_0 is the initial borehole radius. Simplifying this equation and neglecting the higher-order terms gives

$$\frac{R_i}{R_{p,\max}} = \left(\frac{R_0^2}{R_{p,\max}^2} + \frac{(C_u + \frac{3}{2}(K_0 - 1)P_0)}{G}\right)^{\frac{1}{2}} \tag{17}$$

and substituting equation (17) into equation (14) leads to

$$P_i = C_u + \frac{1}{2}(3K_0 - 1)P_0 - C_u \ln\left(\left(\frac{R_0}{R_{p,\max}}\right)^2 + \left(\frac{C_u + \frac{3}{2}(K_0 - 1)P_0}{G}\right)\right) \quad \text{for } K_0 < 1. \tag{18}$$

When $K_0 > 1$, the maximum plastic zone develops adjacent to the spring-line, and an approach similar to that outlined above can be used to obtain the equivalent limiting pressure equation

$$P_i = C_u + \frac{1}{2}(3 - K_0)P_0 - C_u \ln\left(\left(\frac{R_0}{R_{p,\max}}\right)^2 + \left(\frac{C_u + \frac{3}{2}(1 - K_0)P_0}{G}\right)\right) \quad \text{for } K_0 > 1. \quad (19)$$

4. Finite-element evaluation

The effectiveness of equations (18) and (19) for estimating the relationship between the maximum radius of the plastic zone and the applied mud pressure has been evaluated using AFENA (Carter 1992), a non-linear finite-element analysis program which can consider non-hydrostatic initial geostatic stress conditions (i.e. $K_0 \neq 1$). The problem was modelled assuming plane strain and undrained conditions. A mesh composed of a total of 2580 six-noded triangular elements was used. Shear failure and the elastic–plastic constitutive response were modelled using the Mohr–Coulomb failure criterion, total stresses, and undrained strength and deformation parameters.

Mud pressure was applied to the inside surface of the borehole in a number of load increments, and the growth of the plastic zone around the borehole was examined as the internal applied mud pressures were increased. A borehole of diameter 0.4 m at depths of 2 m and 4 m was studied at six different lateral earth pressure coefficients at rest (i.e. K_0 values of 0.75, 0.85, 1, 1.2, 1.4, and 1.6). The parameters used in the analysis are listed in table 1. The mud pressures were adjusted to simulate an increasing column of mud over the borehole (the local gradient within the borehole was kept fixed).

Figure 3 shows the development of the plastic zone around the borehole as the applied mud pressure increases for $K_0 < 1$ (i.e. $K_0 = 0.85$). As the mud pressure increases, the plastic zone grows around the borehole after initial yield. When the mud pressure is about 1.5 times the initial stress P_0, shear failure initiates around the borehole. With further increases in mud pressure, the plastic radius grows steadily around the borehole. Up to mud pressures of $3P_0$, the maximum plastic radius occurs at a point directly over the crown. Once mud pressure reaches $3.5P_0$, the point of shear failure which is furthest from the cavity deviates from above the crown and accelerates towards the ground surface.

Figure 4 shows the development of the plastic zone around the borehole as applied mud pressure increases for $K_0 > 1$ (i.e. $K_0 = 1.4$). The development of the plastic zone around the borehole exhibits characteristics similar to those observed with $K_0 = 0.85$. After initial yield, the plastic zone grows steadily as the mud pressure increases, and the maximum plastic zone appears adjacent to the spring-line. Once the mud pressure P_i exceeds $3.5P_0$, the furthest shear failure point moves around past the shoulder of the borehole and it rapidly extends up to the ground surface.

Table 1. Parameters used in the analysis

Borehole diameter D	0.4 m
Borehole cover depth H	2 and 4 m
Soil unit weight γ_{soil}	20 kN/m^3
Drilling mud unit weight γ_{mud}	13 kN/m^3
Coefficient of lateral earth pressure at rest K_0	0.75, 0.85, 1, 1.4, and 1.6
Undrained cohesion C_u	20, 24, 40, and 60 kPa
Undrained elastic modulus E_u	15 and 25MPa
Poisson's ratio ν	0.49999

Figures 5 and 6 show the radius of the zone of shear failure $R_{p,max}$, normalized using the initial borehole radius R_0, versus the mud pressure P_i, normalized using the mean initial ground stress P_0 at the crown of the borehole. Results are given for cover depths of 2 and 4 m and several K_0 values. Table 2 presents comparisons of the results from the three different solution methods. Results are included for the extent of the plastic zone corresponding to three different distances from the borehole.

- When it extends halfway to the ground surface: $R_{p,max}/R_0 = 5$ (the design limit recommended by Arends (2003)).
- When it extends all the way to the ground surface: $R_{p,max}/R_0 = 11$ (the point where blowout would be expected).
- When the new approach indicates that the plastic zone diverges rapidly (this result is only calculated using the closed-form cavity expansion solutions; since the finite-element solution explicitly models the ground surface, it cannot provide solutions for the plastic zone beyond that point). This pressure P_∞ is also called the 'limiting mud pressure'.

Figure 5 indicates that the new approach works better than the Delft equation at lower load levels (where the mud pressure is less than 80% of the limiting mud pressure), providing improved estimates of maximum plastic radius as a function of borehole mud pressure wherever the earth pressure coefficient K_0 is less than unity (values of 0.75 or 0.85). When $K_0 = 1$, the new procedure provides results identical to the Delft equation, and they both fit the finite-element results well. In the case where $K_0 > 1$, the new procedure also provides a more accurate estimate of the relationship between mud pressure and the extent of the plastic zone. The new procedure also avoids the excessive (unsafe) estimates of mud pressure that arise from the Delft equation once the plastic radius extends beyond two-thirds of the distance towards the ground surface (for both $K_0 < 1$, and $K_0 > 1$).

The comparisons in table 2 show that the new approach gives lower (more conservative) values of limiting mud pressure than the Delft solution when $K_0 \leq 0.75$. For $K_0 > 0.75$, both equations provide essentially the same limiting mud pressure (when the plastic radius diverges). The pressures obtained using the new approach are up to 3% more conservative than the finite-element results. For cases with $K_0 < 1$, the Delft equation overestimates mud pressures by up to 15%. Stress factor is defined as a measure of the additional pressure capacity available once the plastic zone stretches halfway to the ground surface. Values of between 1.2 and 1.29 (a function of K_0) imply 20–30% reserve capacity once the recommended mud pressure limit is reached.

Figure 6 shows that for deeper boreholes (i.e. depth of 4 m) the new solution also produces estimates of the radius of the plastic zone that are more consistent with the finite-element calculations. For problems with non-hydrostatic initial stress ($K_0 \neq 1$), the results from the new approach are very similar to

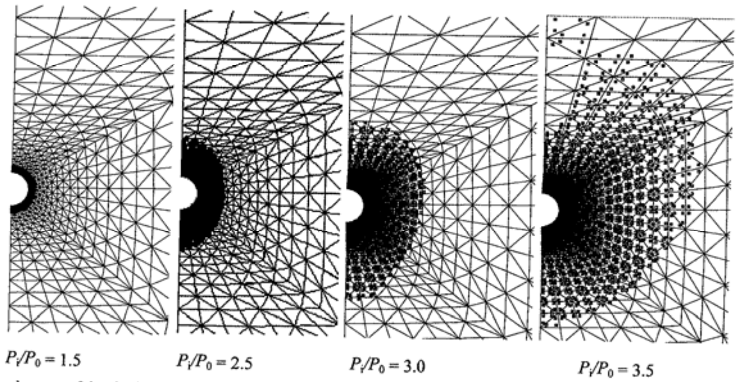

Figure 3. Development of the plastic zone with increasing mud pressure: diameter, 0.4 m; cover depth, 2 m; $K_0 = 0.85$; $C_u d = 20$ kPa; $\gamma = 20$ kN/m^3.

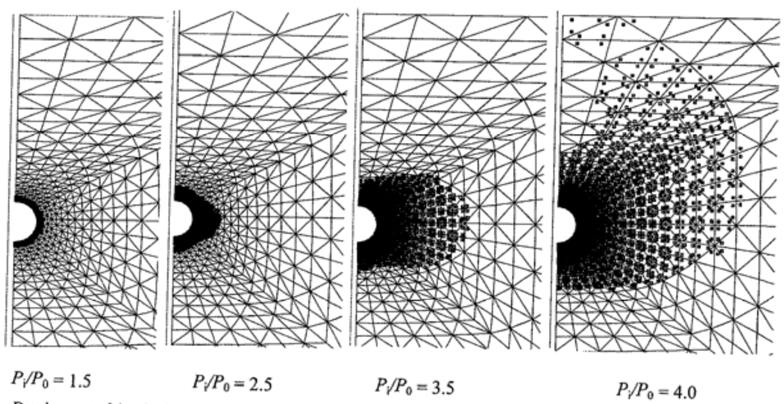

Figure 4. Development of the plastic zone with increasing mud pressure: diameter, 0.4 m; cover depth, 2 m; $K_0 = 1.4$; $C_u = 24$ kPa; $\gamma = 20$ kN/m^3.

the finite-element results when the applied mud pressure is less than 85 percent of the limiting pressure. However, once mud pressures exceed that pressure, the results from the two equations do not fit the finite-element results. This is interpreted as the effect of the ground surface, since it is explicitly considered in the finite-element calculation. In each case, the new approach gives exactly the same results as the Delft equation when $K_0 = 1$, and they fit the finite-element results well. The new approach also performs better than the Delft equation for the case of $K_0 > 1$ and $C_u/P_0 = 0.75$.

5. Limiting mud pressure and the governing mud loss mechanism

Figures 7, 8, and 9 show the relationship between limiting mud pressure and the lateral earth pressure coefficient K_0. Each figure shows maximum mud pressure based on the tensile failure (Kennedy *et al.* 2004a) and blowout cases (equations (18) and (19)), which are collectively denoted the Queen's equation. The range of K_0 values where these blowout or hydrofracture cases apply are marked. Figures 7, 8, and 9 feature undrained cohesions C_u/P_0 of 0.1, 0.5, and 0.7, respectively. Each figure also shows limiting pressures calculated using equation (2) (the Delft equation).

For the specific material in figure 8 (i.e. $C_u/P_0 = 0.5$), the lateral earth pressure coefficient at rest (and therefore the stress history of the clay deposit) controls whether hydraulic fracturing or blowout is expected. When the lateral earth pressure coefficient at rest is less than 0.67 or greater than 2.0, tangential stresses at the crown or spring-line, respectively, become negative (tensile) and hydraulic fracturing is expected to be the governing cause of mud loss during drilling. In this range, the maximum allowable mud pressure is

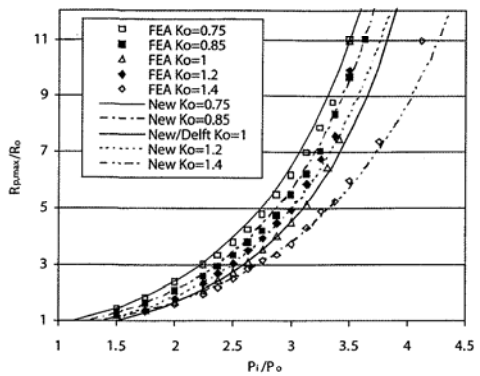

Figure 5. Comparison of the extent of the plastic zone calculated using the Delft equation, the new equation, and finite-element analysis for five different initial stress conditions: K_0 values of 0.75, 0.85, 1, 1.2, and 1.4 (borehole diameter, 0.4 m; cover depth, 2 m; γ= 20 kN/m^3; C_u = 20 kPa (C_u = 24 kPa for K_0 = 1.4)).

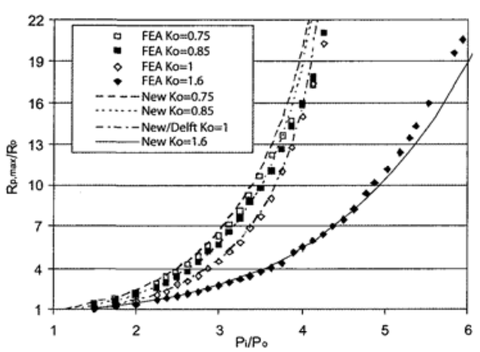

Figure 6. Comparison of the extent of the plastic zone calculated using the Delft equation, the new equation, and finite-element analysis for four different initial stress conditions: K_0 values of 0.75, 0.85, 1.0, and 1.6 (borehole diameter, 0.4 m; cover depth, 4 m; γ= 20 kN/m^3; C_u = 40 kPa (C_u = 60 kPa for K_0 = 1.6)).

estimated using the approach of Kennedy *et al.* (2004a) (equations (18) and (19)).

However, when the lateral earth pressure coefficient at rest is between 0.67 and 2.0, shear failure occurs before the tangential stresses become tensile and the tangential stress subsequently increases with increasing mud pressure (discussed in detail by Kennedy *et al.* 2004a,b). In this case hydraulic fracturing is not expected to occur. Rather, blowout develops at mud pressures that can be estimated using the new procedure reported in this paper. The Delft equation overestimates allowable mud pressure except when K_0 = 1.

Kennedy *et al.* (2004b) developed the following criteria for judging whether hydraulic fracturing or blowout is critical for a given value of K_0:

$$F_1(K_0, P_0, C_u) = \frac{1}{2}(3K_0 - 1)P_0 - C_u \quad \text{for } K_0 < 1. \qquad (20a)$$

$$F_2(K_0, P_0, C_u) = \frac{1}{2}(3 - K_0)P_0 - C_u \quad \text{for } K_0 > 1. \qquad (20b)$$

For a given K_0, if the function is negative for a specific cover depth and shear strength, hydraulic fracturing is expected. If function F is positive, blowout is expected.

Ladd *et al.* (1971) reported that the ratio of shear strength to effective vertical stress (C_u/P_0') was between 0.2 and 0.28 for normally consolidated (NC) clays, between 0.5 and 1.0 for lightly overconsolidated (LOC) clays, and might be larger than 1.2 for heavily overconsolidated (HOC) clays. Assuming that the groundwater table is located at the ground surface and using typical values of soil unit weight, the values of C_u/P_0 (total overburden stress) will be between 0.1 and 0.14 for NC materials, between 0.25 and 0.5 for lightly overconsolidated soils, and over 0.6 for heavily overconsolidated clay. Based on equations (20a) and (20b), hydraulic fracturing will occur in NC clay if K_0 < 0.43, in LOC clay if K_0 < 0.67, and in HOC clay if K_0 > 1.8.

Now, typical values of K_0 for NC clay range from 0.5 to 0.6, for LOC clay K_0 is close to unity, and for HOC clay $K_0 \geq 3$. Therefore it appears that NC and LOC clays are most susceptible to blowout. Hydraulic fracturing is expected in HOC clay once K_0 exceeds 1.8, while blowout is expected at lower K_0 values.

Table 2. Comparisons of stress ratios estimated using the three different solutions (cover depth, 2 m; diameter, 0.4 m)

K_0	P^5_{Delft}/P^5_{New}	$P^{11}_{Delft}/P^{11}_{New}$	$P^{\infty}_{Delft}/P^{\infty}_{New}$	P^5_{New}/P^5_{FEA}	$P^{11}_{New}/P^{11}_{FEA}$	Stress factor
0.75	1.15	1.04	0.95	0.97	1.0	1.29
0.85	1.1	1.04	1.0	0.99	0.97	1.25
1.0	1.0	1.0	1.0	0.99	1.0	1.2
1.2	1.1	1.05	0.88	1.0	0.98	1.26
1.4	1.1	1.02	0.93	1.0	0.98	1.28

P^B_A: subscript A = Delft, New, or FEA denotes the three different solutions; superscript B = 5, 11, or ∞ denotes the distance the plastic zone extends (corresponding to halfway to the surface, all the way to the surface, and a very large distance).
Stress factor = P^5_{New}/P^{11}_{New} (pressure ratio for plastic zone halfway and all the way to the surface).

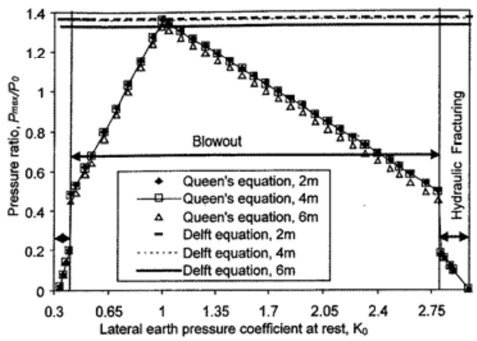

Figure 7. Relationship between pressure ratio (ratio of applied mud pressure to initial overburden pressure) and lateral earth pressure coefficient K_0 (normally consolidated clay, $C_u/P_0 = 0.1$).

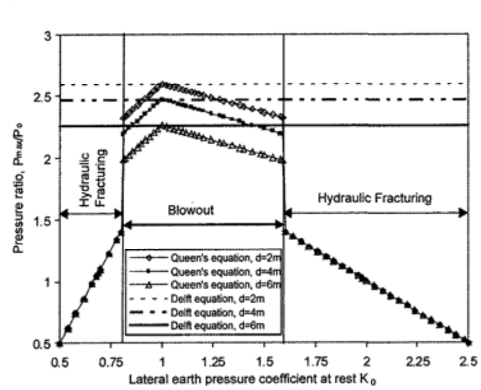

Figure 9. Relationship between pressure ratio (ratio of applied mud pressure to initial overburden pressure) and lateral earth pressure coefficient K_0 (heavily overconsolidated clay, $C_u/P_0 = 0.7$).

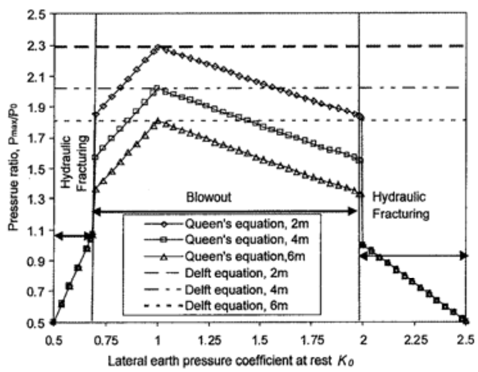

Figure 8. Relationship between pressure ratio (ratio of applied mud pressure to initial overburden pressure) and lateral earth pressure coefficient K_0 (lightly overconsolidated clay, $C_u/P_0 = 0.5$).

6. Summary and conclusions

Control of maximum mud pressure to prevent mud loss during directional drilling is recognized as an important issue during project design and construction. Two mechanisms causing ground failure have been reviewed, namely hydraulic fracture and shear failure. A new approach for estimating the maximum allowable mud pressure, which considers growth of maximum plastic radius with increasing mud pressure, has been reported. The procedure explicitly considers coefficients of lateral earth pressure that are not equal to unity. Finite-element calculations were used to examine the effectiveness of the new approach. Comparisons were made of the size of the plastic zone surrounding the borehole (where shear failure has occurred) obtained using the new approach, the Delft equation, and the finite-element calculations. These demonstrate that, when initial ground stress conditions are not isotropic, the new approach provides estimates of the radius of the plastic zone that more closely match the finite-element calculations than do estimates obtained using the Delft equation. The new approach still neglects interaction between the borehole and the ground surface, and this eventually influences the results when the plastic zone approaches the ground surface.

Maximum mud pressure to prevent mud loss due to hydraulic fracturing can be estimated using the procedure described by Kennedy *et al.* (2004a,b). However, if shear failure develops in the vicinity of the borehole, blowout is the most likely failure mechanism and the dependence of the maximum mud pressure on K_0 can be estimated using the new approach. In the absence of contrary experimental or field evidence, allowable borehole pressures can be estimated for the situation where the plastic zone stretches halfway to the ground surface (providing 20–30% reserve capacity). Projects where mud loss would be particularly hazardous should probably employ lower mud pressures.

The parameters used in these calculations should be estimated by experienced geotechnical engineers. Preliminary values for cohesive strength and the coefficient of lateral earth pressure at rest indicate that blowout is the dominant failure mechanism in normally consolidated and lightly overconsolidated clays. Tensile fracture is expected in heavily overconsolidated clays where the coefficient of lateral earth pressure exceeds 1.8. While the new approach presented here has been derived through careful consideration of the relevant soil behaviour, it is theoretical in nature, and both field and laboratory studies would provide valuable guidance on the performance of this analytical method.

Acknowledgements

The work reported here has been supported by the Natural Sciences and Engineering Research Council through the award of a Strategic Research Grant on pulled in place pipe installation.

References

Allouche, E.N., Ariaratnam, S.T., and Biggar, K.W., Environmental remediation using horizontal directional drilling: applications and modelling. *Practice Period. Hazard. Toxic Radioact. Waste Manage.*, 1998, **2**(3), 93–99.

Andersen, K.H., Rawling, G.G., Lunne, T.A., and By, T.H., Estimation of hydraulic fracturing pressure in clay. *Can. Geotech. J.*, 1994, **31**, 817–828.

Arends, G., (2003) Need and possibilities for a quality push within the technique of horizontal directional drilling, in *Proceedings of 2003 No-Dig Conference*, 2003.

Ariaratnam, S.T., and Allouche, E.N., Suggested practices for installations using horizontal directional drilling. *Practice Period. Struct. Design Construct.*, 2000, **5**(4).

Bjerrum, L., Nash, J.K.L., Kennard, R.M., and Gibson, R.E., Hydraulic fracturing in field permeability testing. *Geotechnique*, **22**, 319–332.

Carter, J.P., PROGRAM AFENA: a general finite element algorithm, University of Sydney, 2002.

Carter, J.P., Booker, J.R., and Yeung, S.K., Cavity expansion in cohesive frictional soils. *Geotechnique*, 1986, **36**(3), 349–358.

Kennedy, M.J., Skinner, G.D., and Moore, I.D., Elastic calculations of limiting mud pressures to control hydrofracturing during HDD, in *Proceedings of the 2004 No-Dig Conference*, 2004a.

Kennedy, M.J., Skinner, G., and Moore, I.D., Limiting mud pressures to control hydrofracturing during HDD in an elasto-plastic soil, in *57th Canadian Geotechnical Conference*, 2004b.

Keulen, B., Maximum allowable pressures during horizontal directional drillings focused on sand, Faculty of Civil Engineering and Geosciences, Technical University Delft, 2001.

Ladd, C.C., Poulos, H.G., and D'Appolonia, D.J., Initial settlement of structures on clay. *J. Soil Mech. Found. Div. ASCE*, 1971, **97**(SM10), 1359–1377.

Moore, I.D., Analysis of ground fracture due to excessive mud pressure *Proceedings of the 2005 No-Dig Conference*, 2005.

Mori, A., and Tamura, M., Hydrofracturing pressure of cohesive soils. *Soils Found.*, 1987, **27**(1), 14–22.

Murdoch, L.C., Hydraulic fracturing of soil during laboratory experiments: methods and observations. *Geotechnique*, 1993a, **43**(2), 255–265.

Murdoch, L.C., Hydraulic fracturing of soil during laboratory experiments: propagation. *Geotechnique*, 1993b, **43**(2), 266–276.

Murdoch, L.C., Hydraulic fracturing of soil during laboratory experiments: theoretical analysis. *Geotechnique*, 1993c, **43**(2), 276–287.

Murdoch, L.C., Mechanical analysis of idealized shallow hydraulic fracture, *J. Geotech. Geoenviron. Eng.–ASCE*, 2002, **128**(6), 488–495.

Panah, A.K., and Yanagisawa, E., Laboratory studies on hydraulic fracturing criteria in soil. *Soils Found.*, 1989, **29**(4), 14–22.

Vesic, A.S., Expansion of cavities in infinite soil mass. *Journal of Soil Mechanics and Foundations Division*, 1972, **98**(SM3), 265–290.

Yu, H.S., *Cavity Expansion Methods in Geomechanics*, 2000 (Dordrecht: Kluwer Academic).